Journal of Marine Research, 42, 473–485, 1984

Journal of
MARINE RESEARCH

Volume 42, Number 3

An analytic model of tidal waves in the Yellow Sea

by Yong Q. Kang [1]

ABSTRACT

Co-oscillating tides in the Yellow Sea south of Shantung Peninsula are investigated analytically by a superposition of Kelvin and Poincaré waves. The Yellow Sea is approximated by a rectangular bay of uniform depth with an opening at the head, and a variable portion of tidal energy is allowed to penetrate through the opening. The analytical results basically agree with the available tidal charts. For the semi-diurnal tide the Poincaré waves play an important role throughout the whole basin of the Yellow Sea, but for the diurnal tide their influence is restricted to the vicinity of the bay head. The asymmetry of amphidromic system arises primarily due to a partial penetration of tidal energy through the opening at the bay head. A large tidal elevation in the Kyunggi Bay south of Ongjin Peninsula is due to the modifications of Kelvin and Poincaré waves at the Ongjin Peninsula.

1. Introduction

The tides in the Yellow Sea and the East China Sea are rather well understood by analysis of tidal records (Ogura, 1933) and by hydro-numerical tidal models (An, 1977; Choi, 1980; Kagan *et al.*, 1966). Ogura's (1933) tidal charts of the Yellow Sea are shown in Figure 1. The amphidromic points in the Yellow Sea south of Shantung Peninsula are located near China, and the tidal ranges in the eastern part of the Yellow Sea (near Korea) are larger than those in the western part (near China). The asymmetric distribution of tidal ranges is also evident in the numerically computed tidal chart by Choi (1980), shown in Figure 2.

We can, in principle, have a realistic description of tides in the Yellow Sea by means of a hydro-numerical tidal model. However, the analytic model developed in this paper is very useful since it provides insights to the observed tidal phenomena.

1. Department of Oceanography, National Fisheries University of Pusan, Pusan 608, Korea.

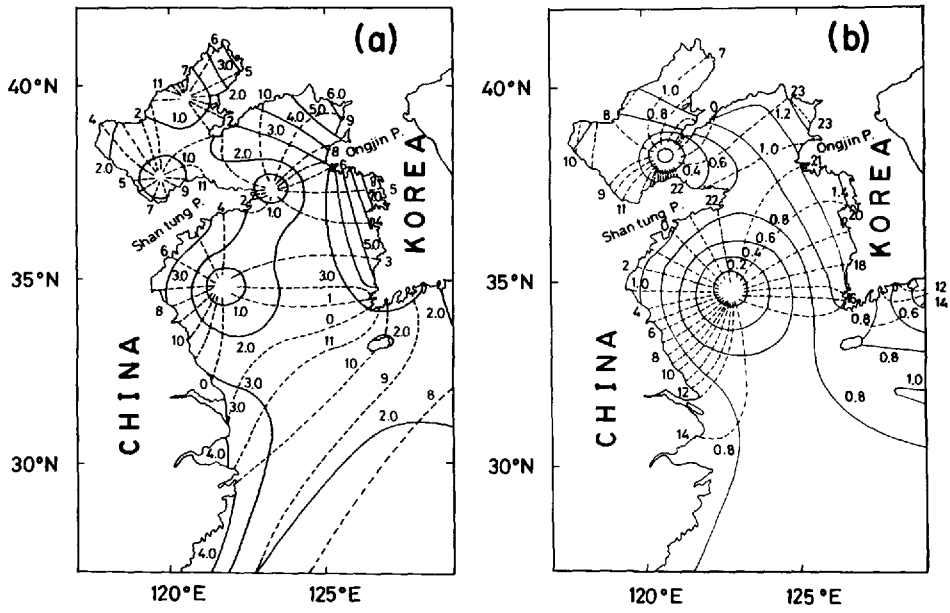

Figure 1. Tidal charts in the Yellow Sea and the East China Sea (after Ogura, 1933). (a) Co-tidal lines of M_2 tide referred to 135E and spring co-range lines, $2(M_2 + S_2)$, in meters. (b) Co-tidal lines of K_1 tide referred to 135E and spring co-range lines, $2(K_1 + O_1)$, in meters.

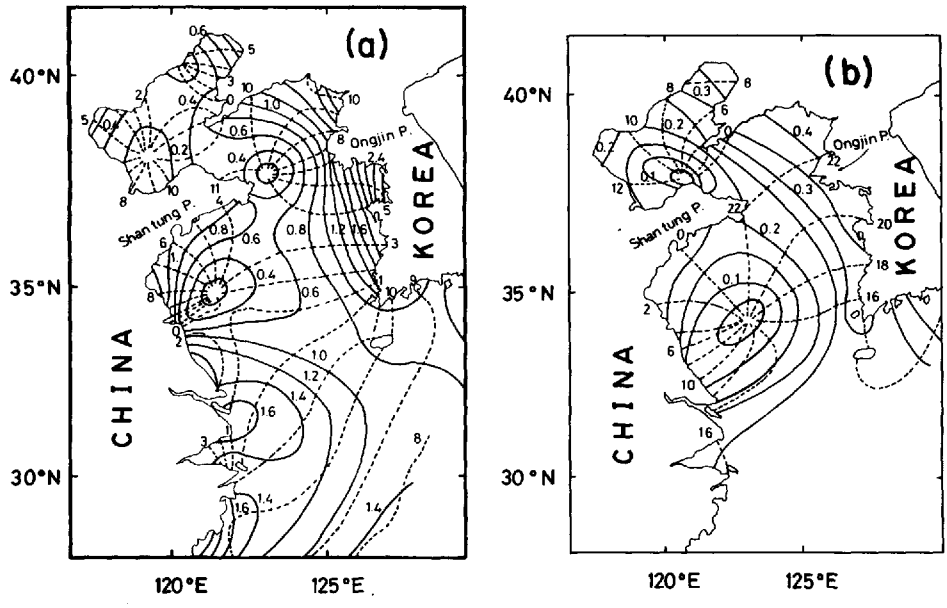

Figure 2. Computed tidal charts of (a) M_2 and (b) K_1 tides in the Yellow Sea and the East China Sea (after Choi, 1980).

The analytic solution for tidal waves in a rotating rectangular bay of uniform depth was first obtained by Taylor (1921; see Defant, 1961, pp. 202–219). Taylor's solution consists of a linear superposition of incident and reflected Kelvin waves and an infinite number of Poincaré waves. The amphidromic points are located on the central axis of the rectangular bay, and the tidal ranges are symmetric with respect to the central axis. Since the amphidromic system in the Yellow Sea is asymmetric, we need a more realistic model that explains the origin of the asymmetry.

Hendershott and Speranza (1971) showed that the Poincaré waves decay rapidly with distance from the head of a sufficiently narrow and deep bay, and the co-oscillating tides in such a bay consist of Kelvin waves. They showed that an asymmetry of amphidromic system in such a bay results from a partial absorption of incident power flux at the bay head. However, since the Yellow Sea with a typical depth of 50 m and width of 600 km is not so narrow and deep, we cannot neglect the Poincaré waves in the Yellow Sea. In other words, a superposition of oppositely travelling Kelvin waves without inclusion of Poincaré waves is not suitable for a realistic model of tidal waves in the Yellow Sea.

Brown (1973) showed that an asymmetry of amphidromic system is possible in a rectangular bay, even though there is no loss of energy, provided that the tidal period is shorter than the critical period of the first Poincaré mode. The critical period in a rectangular bay of 600 km wide and 50 m deep located at 36N is 12.1 hours (see (2.8)), slightly shorter than the semi-diurnal tidal period of 12.42 hours. In the Yellow Sea, the concept of the critical period cannot explain the asymmetry of diurnal tide, the period of which is about two times longer than the critical period.

Rienecker and Teubner (1980) showed that the energy dissipation by bottom friction generates an asymmetry of amphidromic system in a rectangular bay. The Yellow Sea can be approximated by a rectangular bay the head of which has an opening as shown in Figure 3. The energy losses due to bottom friction and due to a penetration of wave energy through the opening are expected to be responsible for the asymmetry of amphidromic system in the Yellow Sea. In this paper, through an analytic model of co-oscillating tides, we want to understand the roles of the Shantung and the Ongjin Peninsulas on the tidal waves in the Yellow Sea. For mathematical simplicity, we assume a flat bottom and neglect bottom friction in the model.

2. Governing equation

Linearized long wave equations in a rotating basin of constant depth are

$$\begin{aligned} \frac{\partial u}{\partial t} - fv &= -g\frac{\partial \zeta}{\partial x} \\ \frac{\partial v}{\partial t} + fu &= -g\frac{\partial \zeta}{\partial y} \\ \frac{\partial \zeta}{\partial t} + H\left(\frac{\partial u}{\partial x} + \frac{\partial v}{\partial y}\right) &= 0, \end{aligned} \tag{2.1}$$

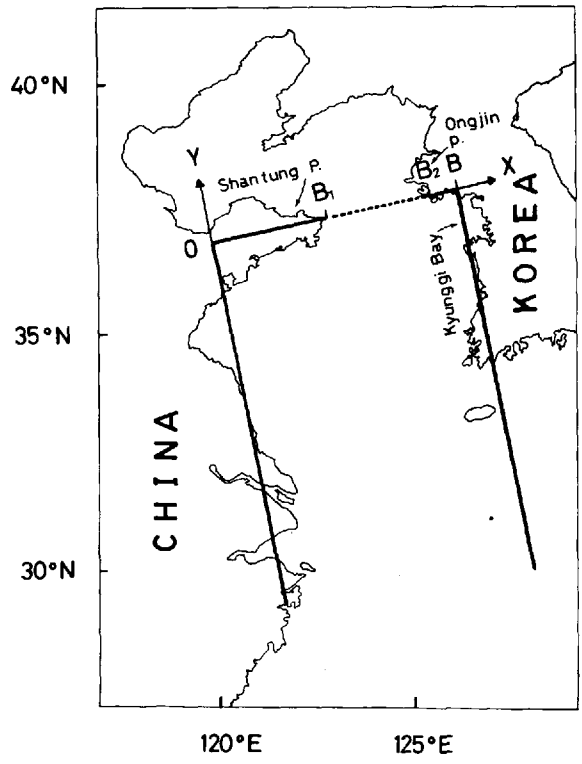

Figure 3. A rectangular bay of 600 km wide with an open boundary of 200 km long at the head.

where u and v are depth-averaged velocities to the x (east) and y (north) directions, respectively, f the Coriolis parameter, g the gravity, ζ the sea level elevation from the mean sea level, and H mean depth of the basin. In (2.1) we neglect tide generating force and bottom friction.

The appropriate kinematic boundary condition along a coastal line with a vertical wall is

$$\mathbf{v} \cdot \mathbf{n} = 0, \tag{2.2}$$

where $\mathbf{v} = (u, v)$ and $\mathbf{n}$ is a unit vector normal to the coastline. This boundary condition is suitable along the solid boundaries (solid lines in Fig. 3). Along the open boundary at the bay head (dotted boundary in Fig. 3) we may use the boundary condition suggested by Proudman (1941)

$$v = \frac{\sqrt{gH}}{H}\zeta = \alpha\zeta \text{ at } y = 0. \tag{2.3}$$

If $\alpha = 0$, then (2.3) becomes identical to (2.2). At the head of the rectangular bay ($y = 0$) we use (2.3) with $\alpha = 0$ along the solid boundary ($0 \le x \le B_1$, $B_2 \le x \le B$) and $\alpha = \sqrt{gH}/H$ along the open boundary ($B_1 < x < B_2$).

Co-oscillating tides in a rectangular bay consist of Kelvin and Poincaré waves. Kelvin waves in a bay with width B and depth H are described by

$$\begin{aligned} u &= 0 \\ v &= \frac{g}{c} A_0[e^{(x-B)/r} e^{il_0 y} - Re^{-x/r} e^{-il_0 y}]e^{-i\omega t} \\ \zeta &= A_0[e^{(x-B)/r} e^{il_0 y} + Re^{-x/r} e^{-il_0 y}]e^{-i\omega t}, \end{aligned} \tag{2.4}$$

where A_0 is the amplitude of sea-level elevation at the right wall ($x = B$) associated with the incident (or northward propagating) Kelvin wave, R is the reflection coefficient of Kelvin wave, l_0 is the meridional wavenumber of the Kelvin wave, ω the frequency, r of the barotropic Rossby radius of deformation defined by

$$r = \frac{\sqrt{gH}}{f} = \frac{c}{f}, \tag{2.5}$$

and $c = \sqrt{gH}$ is the phase speed of the Kelvin wave. Kelvin waves cannot satisfy the boundary conditions at the bay head.

Poincaré waves in an infinite canal ($0 \le x \le B$, $-\infty < y < \infty$) consist of a linear superposition of plane Sverdrup waves subject to boundary conditions $u = 0$ at $x = 0$ and at $x = B$. The sea-level elevation and velocity field associated with Poincaré waves in the canal are (cf, LeBlond and Mysak, 1978, p. 272)

$$\begin{aligned} u &= -\frac{ig}{f^2 - \omega^2} \sum_{m=1}^{\infty} A_m \left(\omega k_m + \frac{f^2 l_m^2}{\omega k_m}\right) \sin k_m x e^{i(l_m y - \omega t)} \\ v &= g \sum_{m=1}^{\infty} A_m \left(\frac{f}{gHk_m} \sin k_m x + \frac{l_m}{\omega} \cos k_m x\right) e^{i(l_m y - \omega t)} \\ \zeta &= \sum_{m=1}^{\infty} A_m \left(\cos k_m x + \frac{f l_m}{\omega k_m} \sin k_m x\right) e^{i(l_m y - \omega t)}, \end{aligned} \tag{2.6}$$

where $m = 1, 2, 3, \ldots$ is the cross-channel mode number of Poincaré waves, A_m the amplitude, and (k_m, l_m) the wavenumber vector of the m-th Poincaré mode defined by

$$\begin{aligned} k_m &= \frac{m\pi}{B} \\ l_m^2 &= \frac{\omega^2 - f^2}{gH} - k_m^2. \end{aligned} \tag{2.7}$$

If the period of the tidal wave is larger than the critical period, T_c, given by

$$T_c = \frac{2\pi}{\sqrt{f^2 + \dfrac{gHm^2\pi^2}{B^2}}}, \tag{2.8}$$

then l_m becomes an imaginary number and the corresponding Poincaré modes will decay exponentially as they propagate southward.

A linear superposition of Kelvin waves and a whole set of Poincaré modes is necessary in order to satisfy the boundary condition at the head of bay. The velocity field and sea-level elevation associated with Kelvin and Poincaré waves are, from (2.4) and (2.6),

$$u = \sum_{m=1}^{\infty} \frac{ig}{\omega^2 - f^2} A_m \left(\omega k_m + \frac{f^2 l_m^2}{\omega k_m}\right) \sin k_m x e^{i(l_m y - \omega t)} \tag{2.9}$$

$$\begin{aligned} v = {} & \frac{g}{c} A_0 [e^{(x-B)/r} e^{il_0 y} - Re^{-x/r} e^{-il_0 y}] e^{-i\omega t} \\ & + \sum_{m=1}^{\infty} g A_m \left(\frac{f}{gHk_m} \sin k_m x + \frac{l_m}{\omega} \cos k_m x\right) e^{i(l_m y - \omega t)}, \end{aligned} \tag{2.10}$$

$$\begin{aligned} \zeta = {} & A_0 [e^{(x-B)/r} e^{il_0 y} + Re^{-x/r} e^{-il_0 y}] e^{-i\omega t} \\ & + \sum_{m=1}^{\infty} A_m \left(\cos k_m x + \frac{f l_m}{\omega k_m} \sin k_m x\right) e^{i(l_m y - \omega t)}. \end{aligned} \tag{2.11}$$

Boundary conditions at the sides of the rectangular bay (i.e., $u = 0$ at $x = 0$ and $x = B$) are satisfied for any values of R and A_m. However, the required boundary condition at the bay head restricts possible values of R and A_m.

3. Method of solution

A method of determining the reflection coefficient of Kelvin wave and the amplitudes of Poincaré waves in rectangular bays with various configurations of the bay head is as follows. The boundary condition (2.3) at the head of the rectangular bay becomes, using (2.10) and (2.11),

$$\begin{aligned} & \frac{g}{c} A_0 (e^{(x-B)/r} - Re^{-x/r}) + \sum_{m=1}^{N} g A_m \left(\frac{f}{gHk_m} \sin k_m x + \frac{l_m}{\omega} \cos k_m x\right) \\ & \qquad = \alpha A_0 (e^{(x-B)/r} + Re^{-x/r}) + \sum_{m=1}^{N} \alpha A_m \left(\cos k_m x + \frac{f l_m}{\omega k_m} \sin k_m x\right), \end{aligned} \tag{3.1}$$

where we truncate the infinite series of Poincaré modes up to a finite mode number N.

This equation can be written as

$$\left(\frac{g}{c}-\alpha\right)A_0e^{(x-B)/r}-\left(\frac{g}{c}+\alpha\right)RA_0e^{-x/r}+\sum_{m=1}^{N}A_mF_m(x)=0, \tag{3.2}$$

where

$$F_m(x)=\frac{f}{Hk_m}\sin k_mx+\frac{gl_m}{\omega}\cos k_mx-\alpha\cos k_mx-\alpha\frac{fl_m}{\omega k_m}\sin k_mx. \tag{3.3}$$

In order to have a southward propagating (or decaying) Poincaré mode, we should have (see (2.7))

$$\begin{aligned} l_m &= -\sqrt{\frac{\omega^2-f^2}{gH}-k_m^2} \quad \text{if} \quad \frac{\omega^2-f^2}{gH}\geq k_m^2, \\ l_m &= -i\sqrt{k_m^2-\frac{\omega^2-f^2}{gH}} \quad \text{if} \quad \frac{\omega^2-f^2}{gH}<k_m^2. \end{aligned} \tag{3.4}$$

For a given amplitude A_0 of the incoming Kelvin wave we can determine the reflection coefficient R and the amplitudes A_m ($m = 1, 2, 3, \ldots, N$) of Poincaré modes by the collocation method introduced by Brown (1973). In the collocation or 'point-matching' method, (3.2) is required to be satisfied at $N + 1$ points along the bay head ($0 \leq x \leq B$). The bay head in Figure 3 consists of solid ($0 \leq x \leq B_1$ and $B_2 \leq x \leq$ B) and open ($B_1 < x < B_2$) boundaries. The inhomogeneity of the required boundary condition at the head, however, can be modelled by assigning different values of α_i corresponding to the positions x_i at the head. Boundary conditions along a vertical wall (i.e., solid boundary) can be modelled by assigning $\alpha = 0$. An application of (3.2) at $N + 1$ points, $x_1, x_2, \ldots, x_{N+1}$, along the northern bay head yields a matrix equation

$$\mathbf{FY} = \mathbf{G}, \tag{3.5}$$

where elements of **F** and **G** are given by

$$\begin{aligned} F_{im} &= F_m(x_i) && (i = 1 \text{ to } N+1,\ m = 1 \text{ to } N) \\ F_{1,N+1} &= -\left(\frac{g}{c}+\alpha_i\right)A_0e^{-x_i/r} && (i = 1 \text{ to } N+1) \\ G_i &= \left(\alpha_i-\frac{g}{c}\right)A_0e^{(x_i-B)/r} && (i = 1 \text{ to } N+1) \end{aligned} \tag{3.6}$$

The solution vector

$$\mathbf{Y} = (A_1, A_2, \ldots, A_N, R) \tag{3.7}$$

yields amplitudes of the Poincaré modes and the reflection coefficient of the Kelvin wave.

Co-tidal and co-range lines are computed as follows. The sea-level elevation (2.11) can be represented as

$$\zeta(x, y, t) = \tilde{\zeta}(x, y) \exp(-i\omega t) = |\tilde{\zeta}(x, y)| \exp[i(\theta - \omega t)] \tag{3.8}$$

where

$$|\tilde{\zeta}(x, y)| = \sqrt{\tilde{\zeta}_r^2 + \tilde{\zeta}_i^2} \tag{3.9}$$

$$\theta(x, y) = \tan^{-1}(\tilde{\zeta}_i/\tilde{\zeta}_r) \tag{3.10}$$

and $\tilde{\zeta}_r$ and $\tilde{\zeta}_i$ are the real and imaginary parts of $\tilde{\zeta}(x, y)$, respectively. Co-range lines are constructed by following lines along which $|\tilde{\zeta}(x, y)|$ is constant. Co-tidal lines are described by curves along which $\theta(x, y) - \omega t = \text{const}$, or

$$t = \theta(x, y)/\omega + \text{const.} \tag{3.11}$$

4. Results

In this paper I present tidal charts in a rectangular bay with three different head configurations. The first configuration has no open boundary at the head. The second configuration consists of a solid boundary of 300 km, an open boundary of 200 km, and another solid boundary of 100 km. The two solid boundaries at the head correspond to the Shantung and the Ongjin Peninsulas (see Fig. 3). The third configuration consists of a solid boundary of 300 km and an open boundary of 300 km. The solid boundary on the right-hand side of the head in the second configuration is replaced by an open boundary in order to study the influence of the Ongjin Peninsula on the co-oscillating tides in the Yellow Sea. For all of the three configurations the bay is assumed to be 600 km wide and 50 m deep, and the Coriolis parameter is evaluated at 36N. The amplitude of the incoming Kelvin wave at the right wall ($x = B$) is assumed to be $A_0 = 10$ m. The boundary condition (2.3) with $\alpha = 0$ and 0.5 sec^{-1} are used along the solid and the open boundaries, respectively, at the bay head. The α of 0 implies no normal flow across the solid boundary, and the α of 0.5 sec^{-1} corresponds to a depth of 50 m at the open boundary.

Figure 4 shows the co-range (solid curve) and co-tidal lines (dotted curve) of co-oscillating semi-diurnal and diurnal tides in a rectangular bay without an open boundary at its head. Since the semi-diurnal tidal period of 12.42 hours and diurnal period of 24.0 hours are larger than the critical period of 12.1 hours of the first Poincaré mode, the reflection coefficient $|R| = 0$ and the amphidromic system is symmetric with respect to the central axis of the bay. The *e*-folding distance of the first Poincaré mode is 4600 km for the semi-diurnal tide and 316 km for the diurnal tide (see (3.4)). Hence, for the diurnal tide the Poincaré waves are restricted to the vicinity

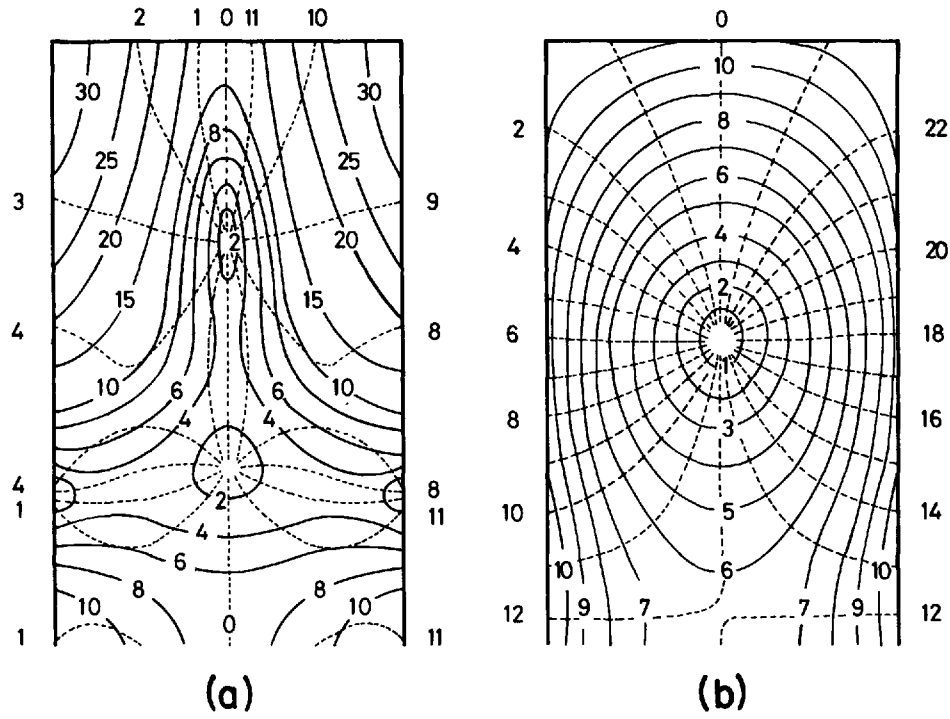

Figure 4. Tidal charts of (a) the semi-diurnal tide with a period of 12.42 hrs and (b) the diurnal tide with a period of 24 hrs in a rectangular bay of 600 km wide, 1000 km long, and 50 m deep. Co-tidal lines of semi-diurnal and diurnal tides are respectively in lunar and in solar hours. The amplitude of incoming Kelvin wave is 10 m on the right wall.

of the bay head, but for the semi-diurnal tide the Poincaré waves give a substantital influence throughout the Yellow Sea.

Figure 5 shows tidal charts in a rectangular bay which has an open boundary of 200 km at its head. Since a part of the tidal energy flux penetrates through the open boundary at the bay head, the incident Kelvin wave is not completely reflected. The reflection coefficients of Kelvin waves are $|R| = 0.300$ and 0.340 for semi-diurnal and diurnal tides, respectively. For the semi-diurnal tide (Fig. 5a) amphidromic points are found at (240, −260) km and (50, −750) km. The northern amphidromic point agrees reasonably with the amphidromic point in available tidal charts of Figures 1a and 2a, but the southern one does not. For the diurnal tide (Fig. 5b) one amphidromic point is located at (170, −55) km. General distributions of co-range lines in the rectangular bay of Figure 5 agree reasonably with those obtained from the tidal record (Fig. 1) or from a numerical tidal model (Fig. 2). The tidal ranges on the right-hand side of the bay are larger than those on the left-hand side. The origin of the asymmetry of amphidromic system is attributed due to a partial penetration of tidal energy flux through the open boundary at the bay head. The maximum tidal range in Figure 5 is found at the upper

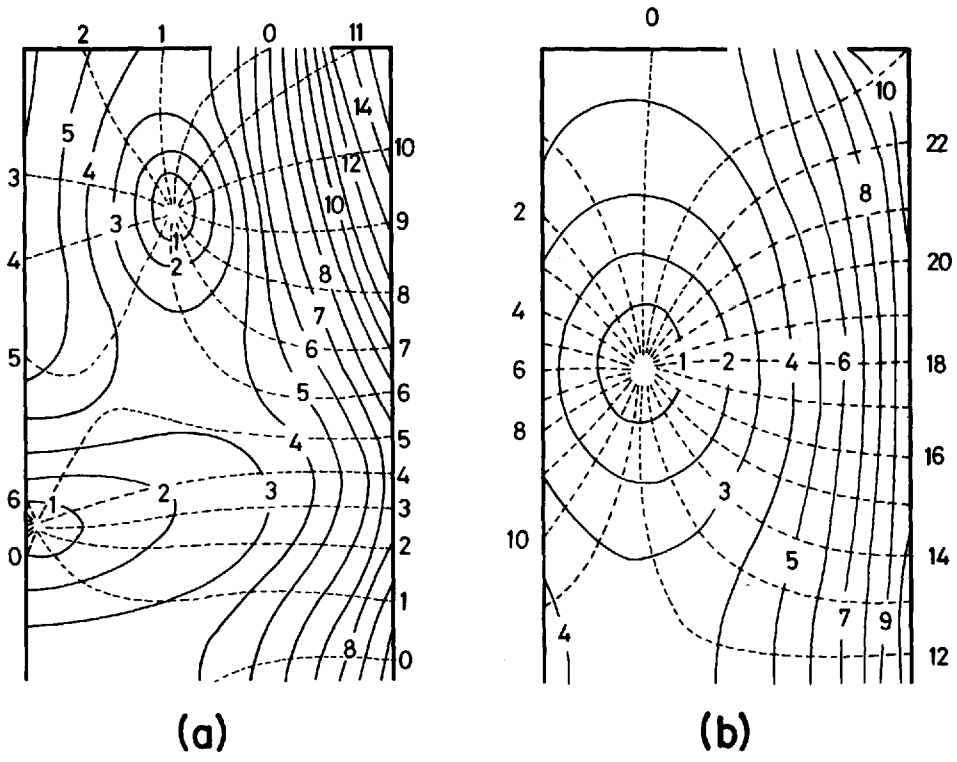

Figure 5. Tidal charts of (a) the semi-diurnal and (b) the diurnal tides in a rectangular bay with an opening at its head. The head consists of a solid boundary of 300 km, an open boundary of 200 km, and another solid boundary of 100 km. Other parameters are the same as in Figure 4.

right corner, and this feature is in agreement with the available tidal maps of Figures 1 and 2. The results with other values of α at the open boundary of the bay head show that the amphidromic points generally shift to the left as the α increases or as more energy penetrates through the opening (results not shown).

Figure 6 shows tidal charts in a rectangular bay with a solid boundary of 300 km and an open boundary of 300 km at its head. The solid boundary of 100 km at the right-hand side of the head in Figure 5 is removed in order to study the influences of the Ongjin Peninsula on the co-oscillating tides in the Yellow Sea. A particularly strong tidal elevation, which was found at the upper right corner of Figure 5, is not found in Figure 6. Since the length of open boundary at the head of Figure 6 is larger than that of Figure 5, one expects that in the bay of Figure 6 more tidal energy penetrates northward through the open boundary at the head than in the bay of Figure 5. In fact, the reflection coefficients $|R| = 0.235$ and 0.180 of semi-diurnal and diurnal tides, respectively, of Figure 6 are smaller than the corresponding values of 0.300 and 0.340 of Figure 5.

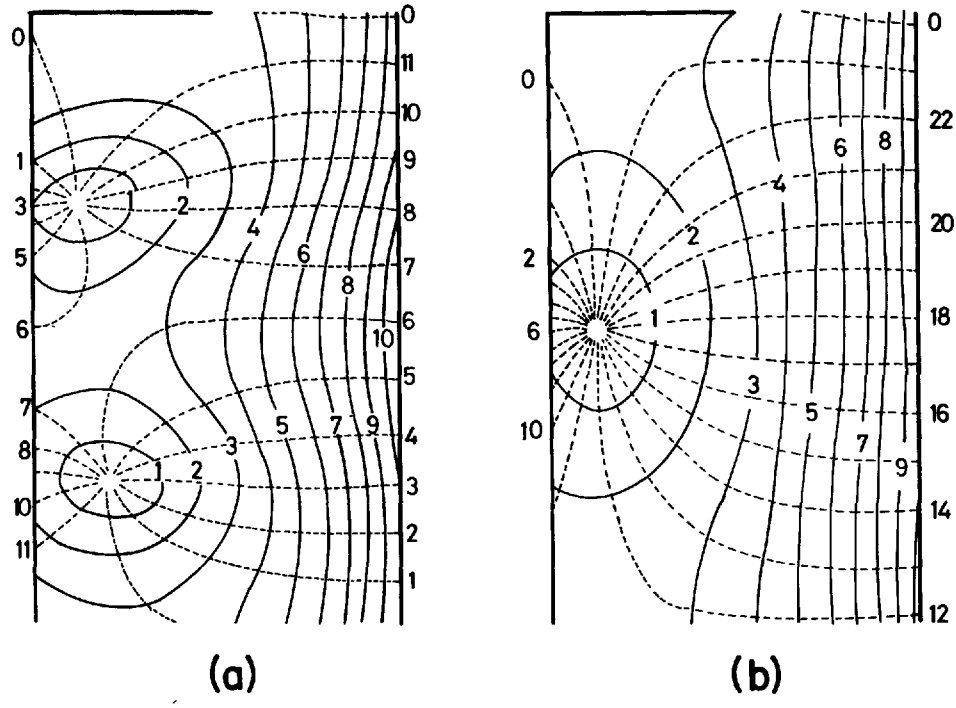

Figure 6. Tidal charts of (a) the semi-diurnal and (b) the diurnal tides in a rectangular bay the head of which consists of a solid boundary of 300 km and an open boundary of 300 km. Other parameters are the same as in Figure 4.

For diurnal tides Poincaré waves decay rapidly with distance from the bay head. The co-oscillating tides in the rectangular bay, except at the vicinity of the head, are described basically by oppositely travelling Kelvin waves. The amplitude of reflected or southward propagating Kelvin wave for diurnal tide in Figure 6b is smaller than that of Figure 5b, and the amphidromic points at (70, −500) km in Figure 6b is displaced westward from the corresponding point at (170, −500) km in Figure 5b. For semi-diurnal tides, however, the Poincaré waves decay very slowly with distance from the head of bay, and therefore their influences are substantial throughout the Yellow Sea. The amphidromic points in Figure 6a are found at (80, −300) km and (130, −740) km. A comparison of Figures 5a and 6a shows that if the Ongjin Peninsula were removed, then the northern amphidromic point would move to the left and the southern one would move to the right.

The Ongjin Peninsula plays an important role in determining the reflection coefficient of Kelvin waves and the amplitudes of Poincaré waves. The different co-oscillating tides shown in Figures 5 and 6 imply that the large tidal elevations in the Kyunggi Bay south of the Ongjin Peninsula are primarily due to the modifications of the Kelvin and Poincaré waves at the Ongjin Peninsula.

5. Discussion and conclusions

In this paper co-oscillating tides in a rectangular bay with different configurations of the bay head are considered in order to have insights on the tidal phenomena in the Yellow Sea. Due to the complexity of coastal geometry in the Yellow Sea, I excluded the northern part (north of Shantung Peninsula) in the analytic model. For mathematical simplicity, I neglected the tidal energy dissipation by bottom friction. The co-oscillating tide in this paper consists of the incoming and reflected Kelvin waves and an infinite number of Poincaré modes. I assume no incoming Poincaré waves, but the Poincaré waves are necessary in order to satisfy the boundary condition at the bay head. Although this model assumes a constant depth, straight coastlines, and vanishing bottom friction, the analytic results (Fig. 5) agree reasonably with available tidal charts of the Yellow Sea. The analytic results give us insights on the roles of the Shantung and Ongjin Peninsulas on the tidal waves in the Yellow Sea. The analytic model shows us the following.

(1) The asymmetric distribution of amphidromic system in the Yellow Sea is primarily due to a partial penetration of tidal energy flux through the strait between the Shantung and the Ongjin Peninsulas. The tidal energy dissipation by bottom friction is also expected to contribute to the asymmetry of the amphidromic system, but this effect is not included in the present study.

(2) The *e*-folding distance for the first mode Poincaré waves in the Yellow Sea is about 300 km for the diurnal tide and a few thousands of kilometers for the semi-diurnal tide. The *e*-folding distances of higher modes are much shorter. Therefore, for diurnal tides Poincaré waves are limited to the vicinity of the Shantung and the Ongjin Peninsulas, but for semi-diurnal tides the Poincaré waves give a significant contribution almost everywhere in the Yellow Sea south of Shantung Peninsula.

(3) The Ongjin Peninsula of about 100 km is very small compared to the wave length of Kelvin waves of 0(1000 km), but the Peninsula plays an important role in the co-oscillating tides in the Yellow Sea. In particular, the Ongjin Peninsula is responsible for large tidal elevations in the Kyunggi Bay south of Ongjin Peninsula.

Acknowledgments. I wish to thank H. J. Lie, H. S. An, and S. H. Kang for helpful comments on this work. Research support by the Korean Science and Engineering Foundation is gratefully acknowledged.

REFERENCES

An, H. S. 1977. A numerical experiment of the M_2 tide in the Yellow Sea. J. Oceanogr. Soc. Japan, *33,* 103–110.

Brown, P. J. 1973. Kelvin-wave reflection in a semi-infinite canal. J. Mar. Res., *31,* 1–10.

Choi, B. H. 1980. A tidal model of the Yellow Sea and the East China Sea. KORDI Rep. 80–02, Korea Ocean Research and Development Institute, Seoul, 72 pp.

Defant, A. 1961. Physical Oceanography, Vol. 2, Pergamon Press, Oxford, 590 pp.

Hendershott, M. C. and A. Speranza. 1971. Co-oscillating tides in long narrow bays; the Taylor problem revisited. Deep-Sea Res., *18,* 959–980.

Kagan, B. A., A. V. Nekrasov and R. E. Tamsalu. 1966. Effects of horizontal friction on tidal sea level oscillation. Bull (Izv.) Acad. Sci. USSR, Atmos. Ocean. Phys., *2,* 174–182.

LeBlond, P. H. and L. A. Mysak. 1978. Waves in the Ocean, Elsevier, Amsterdam, 602 pp.

Ogura, S. 1933. The tides in the seas adjacent to Japan. Hydrogr. Bull. Dep. Imp. Jap. Navy, *7,* 1–189.

Proudman, J. 1941. The effects of coastal friction on the tides. Mon. Not. R. Astr. Soc., Geophys. Suppl., *5,* 23–26.

Rienecker, M. M. and M. D. Teubner. 1980. A note on frictional effects in Taylor's problem. J. Mar. Res., *38,* 183–191.

Taylor, G. I., 1921. Tidal oscillations in gulfs and rectangular basins. Proc. Lond. Math Soc., *30,* 148–181.

Received: *27 May, 1983;* revised: *9 February, 1984.*